Mixing of two-quasineutron and two-quasiproton $K^\pi=6^+$ configurations in the vicinity of ^{174}Yb *

JIAO Chang-Feng(焦长峰)[1] DONG Guo-Xiang(董国香)[1] XU Fu-Rong(许甫荣)[1,2;1)]

[1] State Key Laboratory of Nuclear Physics and Technology, School of Physics, Peking University, Beijing 100871, China
[2] Center for Theoretical Nuclear Physics, National Laboratory for Heavy Ion Physics, Lanzhou 730000, China

Abstract: In the framework of the projected shell model, we investigate the competition between the two-quasineutron and two-quasiproton $K^\pi=6^+$ states in the ytterbium isotopes and $N=104$ isotones adjacent to ^{174}Yb. The ^{174}Yb results are compared with the experimental data. The $K^\pi=6^+$ isomer observed in ^{174}Yb is assigned as an admixture of the $\nu 7/2^-[514]\otimes\nu 5/2^-[512]$ and $\pi 7/2^+[404]\otimes\pi 5/2^+[402]$ intrinsic structure, which explains the experimental $|g_K-g_R|$ value. Similar mixing would appear in ^{172}Yb, ^{176}Hf, and ^{178}W. The low-lying $K^\pi=6^+$ states are also predicted in $^{170\text{-}178}$Yb.

Key words: K isomers, projected shell model, rotational band, g factor

PACS: 27.70.+q, 21.10.Re, 23.20.Lv **DOI:** 10.1088/1674-1137/37/3/034102

1 Introduction

Research on multi-quasiparticle (multi-qp) metastable states provides a unique opportunity to understand the interplay between collective and quasiparticle exciting degrees of freedom in nuclear systems. In particular, an abundance of long-lived high-K isomers (where K is the total angular momentum projection onto the symmetry axis) was found in the $A\sim$170–180 mass region of prolate-deformed nuclei, which has attracted intensive interest both experimentally and theoretically [1–5]. K isomers are of great importance for enhancing the stability of unstable nuclei [6] and novel energy-storage applications [1]. More fundamentally, they offer an insight into the underlying single-particle structure and their pairing strength around the Fermi surface.

In order to study the underlying structural information, a confirmation of the intrinsic structures for K isomers is needed. The gyromagnetic ratio (or g factor) is essential for determining quasiparticle configurations. Recently, a rotational band built on the 830 μs 6^+ isomer in ^{174}Yb has been observed, which makes the g factor measurement accessible for this $K^\pi=6^+$ intrinsic state [7]. Although the $K^\pi=6^+$ state in ^{174}Yb is commonly associated with the $\nu 7/2^-[514]\otimes\nu 5/2^-[512]$ configuration [8], the newly measured g factor shows deviation from the expected value for the two-quasineutron state [7]. This implies that the $K^\pi=6^+$ isomer observed in ^{174}Yb is unlikely to be a "pure" two-quasineutron state. In addition, the existence of both two-quasineutron [9] and two-quasiproton $K^\pi=6^+$ isomers [10] in neighboring nuclei indicates the complexity of the configuration assignment for the 6^+ isomer in this mass region.

The present work aims at a thorough analysis of the two-quasineutron and two-quasiproton $K^\pi=6^+$ states in the $Z=70$ isotopes and $N=104$ isotones adjacent to ^{174}Yb by using the projected shell model (PSM) [11]. As a shell-model-type calculation truncated in the angular-momentum-projected multi-qp basis, the PSM is ideal for studying high-K isomers and the associated rotational bands [5]. Such calculations may shed light on the microscopic origin of high-K multi-qp states by analyzing the wave functions generated in the PSM. Moreover, the well-defined wave functions allow us to compute the g factor, which provides direct indication of dominant multi-qp configurations.

2 The model

In the present calculations, single-particle energies are given by the axially symmetric Nilsson model [12], in which the κ and μ parameters are empirically fitted [13]. The Lipkin-Nogami (LN) pairing [14] has been used in the present PSM calculation. In the PSM, the many-body wave function can be written as a superposition of projected multi-qp states [11, 15]

$$|\Psi_{IM}\rangle=\sum_{K\kappa} f_{IK_\kappa}\hat{P}^I_{MK}|\Phi_\kappa\rangle, \quad (1)$$

Received 5 June 2012
∗ Supported by National Natural Science Foundation of China (10975006)
1) E-mail: frxu@pku.edu.cn

where $\hat{P}^I_{MK}$ is the angular-momentum-projection operator, $|\Phi_\kappa\rangle$ denotes the multi-qp states as a basis set, and f_{IK_κ} is their weight factor. For even-even nuclei, $|\Phi_\kappa\rangle$ consists of the multi-qp states (up to four-qp states) associated with the Nilsson-LN vacuum $|\phi\rangle$:

$$\{|\phi\rangle, a^\dagger_{\nu_1}a^\dagger_{\nu_2}|\phi\rangle, a^\dagger_{\pi_1}a^\dagger_{\pi_2}|\phi\rangle, a^\dagger_{\nu_1}a^\dagger_{\nu_2}a^\dagger_{\pi_1}a^\dagger_{\pi_2}|\phi\rangle\}, \quad (2)$$

where $a^\dagger_\nu$ and $a^\dagger_\pi$ are the creation operators for neutrons and protons, respectively.

The deformed Nilsson-LN states are created with axial symmetry in the present work. Thus each multi-qp state $|\Phi_\kappa\rangle$ has a definite K as a good quantum number. The state of Eq. (1) is a linear combination of various K states, which represents the mixing among different K components. Hence the calculation takes K-mixing effects into account. The energies and wave functions (expressed in terms of f_{IK_κ}) are determined by a variational procedure, i.e., solving the following variational equation [11]

$$\sum_{K'\kappa'}\{H^I_{K\kappa K'\kappa'} - E_I N^I_{K\kappa K'\kappa'}\} f_{IK'_{\kappa'}} = 0, \quad (3)$$

where $H^I_{K\kappa K'\kappa'}$ and $N^I_{K\kappa K'\kappa'}$ are the Hamiltonian and norm matrix elements, respectively.

We employ the total Hamiltonian, which is defined as [11, 16]

$$\hat{H} = \hat{H}_0 - \frac{\chi}{2}\sum_\mu \hat{Q}^\dagger_{2\mu}\hat{Q}_{2\mu} - G_{\rm M}\hat{P}^\dagger\hat{P} - G_{\rm Q}\sum_\mu \hat{P}^\dagger_{2\mu}\hat{P}_{2\mu}, \quad (4)$$

where $\hat{H}_0$ is the spherical Nilsson Hamiltonian. The other terms are standard, i.e., for the quadrupole-quadrupole, monopole-pairing, and quadrupole-pairing interactions, respectively. The strength χ of the quadrupole-quadrupole force is determined by comparison with the deformed Nilsson potential [11]. The monopole-pairing strength $G_{\rm M}$ is determined by the average gap method [17]. The quadrupole-pairing strength $G_{\rm Q}$ is taken to be proportional to $G_{\rm M}$ with a constant of 0.20, which is consistent with the previous PSM calculations [11].

The g factor is ideal for identifying the multi-qp contribution to the wave function. It is defined by

$$g(I) = g_\nu(I) + g_\pi(I), \quad (5)$$

with $g_\tau(I)$ (π for protons and ν for neutrons) given by

$$g_\tau(I) = \frac{1}{\mu_{\rm N}\sqrt{I(I+1)}}[g^\tau_{\rm l}\langle\Psi_{IM}||\hat{j}^\tau||\Psi_{IM}\rangle + (g^\tau_{\rm s} - g^\tau_{\rm l})\langle\Psi_{IM}||\hat{s}^\tau||\Psi_{IM}\rangle], \quad (6)$$

where $|\Psi_{IM}\rangle$ is the wave function of Eq. (1). In the present work, we use the standard values for $g_{\rm l}$ and $g_{\rm s}$ (i.e., $g^\pi_l = 1$, $g^\nu_l = 0$, $g^\pi_{\rm s} = 5.586\times0.75$, and $g^\nu_{\rm s} = -3.826\otimes0.75$). $g^\pi_{\rm s}$ and $g^\nu_{\rm s}$ are both reduced by a quenching factor of 0.75 from the free-nucleon values to account for the core-polarization and meson-exchange current corrections [18].

3 Calculations and discussions

To determine the deformation first, which is needed in the PSM calculations, we calculate the ground-state (g.s.) potential energy surfaces (PESs) by using the Strutinsky method [19], in which the energy is decomposed into macroscopic, quantal shell-correction, and residual pairing energies. The macroscopic energy can be approximated by the standard liquid-drop model [20]. The g.s. deformation can be determined by minimizing the PES. Table 1 lists the calculated quadrupole (ε_2) and hexadecapole (ε_4) deformations for the $Z = 70$ isotopes and $N = 104$ isotones in the vicinity of ^{174}Yb. The calculated quadrupole deformations ε_2 are in good agreement with the experimentally adopted values [21]. In the following PSM calculations, we thus construct the multi-qp basis at the deformations that are listed in Table 1.

Table 1. The quadrupole and hexadecapole deformation parameters for $Z = 70$ isotopes and $N = 104$ isotones.

$Z=70$	^{170}Yb	^{172}Yb	^{174}Yb	^{176}Yb	^{178}Yb
ε_2	0.284	0.287	0.286	0.279	0.274
ε_4	0.034	0.043	0.055	0.064	0.074
$N=104$	^{172}Er	^{174}Yb	^{176}Hf	^{178}W	^{180}Os
ε_2	0.289	0.286	0.271	0.248	0.233
ε_4	0.049	0.055	0.049	0.039	0.040

Figure 1 shows the calculated level spectra for ^{174}Yb, including rotational bands built on different intrinsic structures. It can be seen that the calculated ground-state band, $K^\pi = 6^+$ band, and $K^\pi = 14^+$ band reproduce the experimental data well. Ref. [7] associates the observed $K^\pi = 6^+$ isomer with a two-quasineutron ($\nu7/2^-[514]\otimes\nu5/2^-[512]$) configuration. However, our calculation gives two $K^\pi = 6^+$ bands with nearly degenerate energies. One is based on the $\nu7/2^-[514]\otimes\nu5/2^-[512]$ configuration, and the other is built on a two-quasiproton ($\pi7/2^+[404]\otimes\pi5/2^+[402]$) configuration which lies only 26 keV higher than the two-quasineutron one. Both bands have equivalent rotational behaviors, which are in accord with the experimental $K^\pi = 6^+$ band. Nearly degenerate energies would reinforce the mixing between these two bands. Indeed, mixing of the two-quasiproton and two-quasineutron $K^\pi = 6^+$ bands has been found in neighboring nuclei, ^{176}Hf [22] and ^{174}Hf [10]. However, the extent of the mixing between high-K two-quasineutron and two-quasiproton states is very small in our calculations as well as in previous PSM calculations [23]. This may be related to the model space and the QQ interaction employed in the Hamiltonian of the PSM [23].

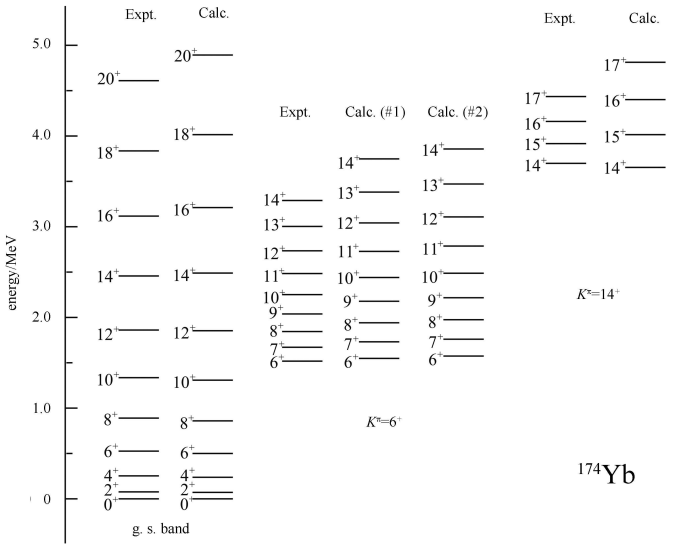

Fig. 1. The calculated level spectra sorted by bands built on different intrinsic structures for ^{174}Yb. The dominant configurations of the prolate high-K bands are K^π=6$^+$(#1): $\nu 7/2^-[514]\otimes\nu 5/2^-[512]$; K^π=6$^+$(#2): $\pi 7/2^+[404]\otimes\pi 5/2^+[402]$; K^π=14$^+$: $\nu 7/2^-[514]\otimes\nu 5/2^-[512]\otimes\pi 9/2^-[514]\otimes\pi 7/2^-[523]$. The experimental data are taken from Ref. [7].

Table 2 lists the calculated g factors for the K^π=6$^+$ states. Our calculation gives g factor values of 0.07 for the two-quasineutron $K^\pi = 6^+$ state and 0.89 for the two-quasiproton $K^\pi = 6^+$ state, respectively. We use $g = g_{\rm R}+(g_{\rm K}-g_{\rm R})\cdot\dfrac{K^2}{I(I+1)}$ and assume $g_{\rm R} = 0.35$ [7] to obtain $|g_{\rm K}-g_{\rm R}| = 0.33(0.63)$ for the two-quasineutron (two-quasiproton) configuration. Experimentally, the observed branching ratios for the $K^\pi = 6^+$ band in ^{174}Yb give a weighted mean of $|g_{\rm K}-g_{\rm R}| = 0.437(6)$ [7], which is higher than the calculated value for the two-quasineutron configuration and is lower than that for the two-quasiproton configuration. The intermediate value of the measured $|g_{\rm K}-g_{\rm R}|$ indicates the mixing of the two K^π=6$^+$ bands. As a consequence of this mixing, one may expect to observe interband transitions between members of the two mixed bands. Further experimental data are needed to clarify this.

Table 2. The calculated g factors for the two-quasineutron and two-quasiproton K^π=6$^+$ states in ^{174}Yb. $g_{\rm R}$ is assumed to be 0.35 [7]. The experimental data are from Ref. [7].

K^π	configuration	g factor (Calc.)	$\lvert g_{\rm K}-g_{\rm R}\rvert$ (Calc.)	$\lvert g_{\rm K}-g_{\rm R}\rvert$ (Expt.)
6$^+$	two-quasineutron	0.07	0.33	0.437(6)
	or			
	two-quasiproton	0.89	0.63	

Systematic observations of the K^π=6$^+$ isomers can be found in $^{172\text{-}178}$Hf [10, 22]. Most of them are dominated by the $\pi 7/2^+[404]\otimes\pi 5/2^+[402]$ configuration, except for ^{176}Hf (N=104), in which the K^π=6$^+$ isomer is an admixture of two-quasiproton and two-quasineutron states [22]. On the contrary, in the $N = 104$ isotones (except ^{176}Hf), the $K^\pi = 6^+$ isomers which have been observed from ^{172}Er to ^{180}Os are associated with the $\nu 7/2^-[514]\otimes\nu 5/2^-[512]$ intrinsic structure [9]. This implies that the two-quasineutron and two-quasiproton structures would compete with each other in this mass region. The competition between these different multi-qp excitations provides useful information about the shell structure of nucleon orbits.

We therefore make a thorough investigation on both two-quasineutron and two-quasiproton $K^\pi = 6^+$ states in the $N = 104$ isotones and $Z = 70$ isotopes. Fig. 2 displays the comparison between the calculated and experimental energies in the $N = 104$ isotones close to ^{174}Yb. Good agreement between the calculations and experiments is obtained for the known $K^\pi = 6^+$ states. Since the $\nu 7/2^-[514]$ and $\nu 5/2^-[512]$ orbits are located around the $N = 104$ neutron Fermi surface, the calculated energies for the two-quasineutron configurations are low and nearly constant. The calculated energies for the two-quasiproton configurations decease rapidly from $Z = 68$ to 72 and increase remarkably from $Z = 72$ to 76. In the range of $Z = 70-74$, the two-quasiproton $K^\pi = 6^+$ state is predicted to be at an energy similar to the two-quasineutron one. This is because of the proton Fermi surfaces of $70 \leqslant Z \leqslant 74$ near the $\pi 7/2^+[404]$ and $\pi 5/2^+[402]$ orbits. Small energy differences may lead to the mixing of the two $K^\pi = 6^+$ states. Accordingly, the $K^\pi = 6^+$ isomers in ^{174}Yb, ^{176}Hf, and ^{178}W would be based on an admixture of the two-quasineutron $\nu 7/2^-[514]\otimes\nu 5/2^-[512]$ and two-quasiproton $\pi 7/2^+[404]\otimes\pi 5/2^+[402]$ intrinsic states.

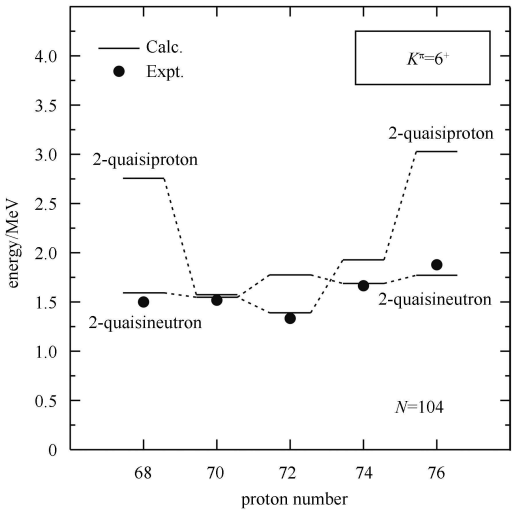

Fig. 2. The energies for the $\nu 7/2^-[514]\otimes\nu 5/2^-[512]$ ($K = 6^+$) and $\pi 7/2^+[404]\otimes\pi 5/2^+[402]$ ($K = 6^+$) states in the $N = 104$ isotones adjacent to ^{174}Yb. The experimental data are taken from Refs. [7, 9, 24].

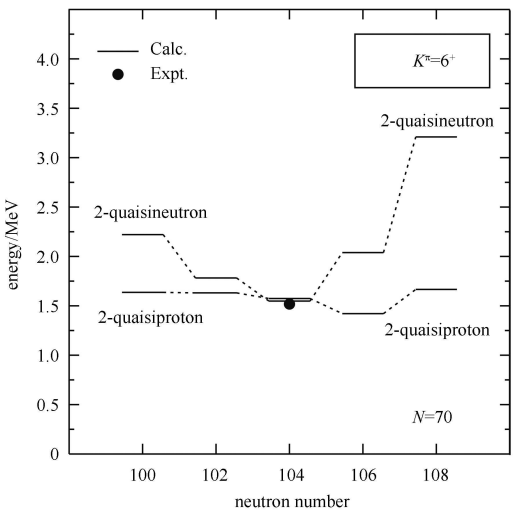

Fig. 3. Similar to Fig. 3, but for the K=6$^+$ states in the ytterbium isotopes adjacent to ^{174}Yb. The experimental data are taken from Ref. [7].

The experimental information concerning the $K^\pi = 6^+$ isomers in ytterbium isotopes is relatively scarce. Our calculations predict the systematic existence of the low-lying K^π=6$^+$ states in $^{170\text{-}178}$Yb. As can be seen in Fig. 3, the calculated energies for the $K^\pi = 6^+$, $\pi 7/2^+[404]\otimes\pi 5/2^+[402]$ states lie at similar energies in $^{170-178}$Yb, whereas the energies for the $\nu 7/2^-[514]\otimes\nu 5/2^-[512]$ states change significantly along with the increasing neutron number. In ^{172}Yb and ^{174}Yb, the two-quasineutron configuration is at a comparable energy to the two-quasiproton one. This may result in serious mixing of these two $K^\pi = 6^+$ states, and a corresponding experimental search is needed.

4 Summary

In summary, we investigated the competition between the two-quasineutron and two-quasiproton $K^\pi = 6^+$ states in the $Z = 72$ isotopes and $N = 104$ isotones in the vicinity of ^{174}Yb by using the projected shell model. The present calculations reproduce the experimental observations well. Our calculation associated the K^π=6$^+$ isomer observed in ^{174}Yb with an admixture of the $\nu 7/2^-[514]\otimes\nu 5/2^-[512]$ and $\pi 7/2^+[404]\otimes\pi 5/2^+[402]$ intrinsic structure, which is supported by the experimental $|g_K - g_R|$ value. Similar mixing would also occur in ^{172}Yb, ^{176}Hf, and ^{178}W. In addition, the systematic existence of the low-lying $K^\pi = 6^+$ states is predicted for $^{170\text{-}178}$Yb.

References

1 Walker P M, Dracoulis G D. Nature (London), 1999, **399**: 35–40
2 Walker P M, Dracoulis G D. Hyperfine Interact., 2001, **135**: 83–107
3 Jain K, Burglin O, Dracoulis G D et al. Nucl. Phys. A, 1995, **591**: 61–84
4 XU F R, Walker P M, Sheikh J A et al. Phys. Lett. B, 1998, **435**: 257–263
5 SUN Y, ZHOU X R, LONG G L et al. Phys Lett B, 2004, **589**: 83–88
6 XU F R, ZHAO E G, Wyss R, Walker P M. Phys. Rev. Lett., 2004, **92**: 252501
7 Dracoulis G D, Lane G J, Kondev F G et al. Phys. Rev. C, 2005, **71**: 044326
8 Borggreen J, Hansen N J S, Pederson J et al. Nucl. Phys. A, 1967, **96**: 561–587
9 Dracoulis G D, Lane G J, Kondev F G et al. Phys. Lett. B, 2006, **635**: 200–206
10 Walker P M, Ward D, Häusser O et al. Nucl. Phys. A, 1980, **349**: 1–9
11 Hara K, SUN Y. Int. J. Mod. Phys. E, 1995, **4**: 637–785
12 Nilsson S G, Tsang C F, Sobiczewski A et al. Nucl. Phys. A, 1969, **131**: 1–66
13 Bengtsson T, Ragnarsson I. Nucl. Phys. A, 1985, **436**: 14–82
14 Pradhan H C, Nogami Y, Law J. Nucl. Phys. A, 1973, **201**: 357–368
15 Ring P, Schuck P. The Nuclear Many Body Problem. New York: Springer, 1980. 473–478
16 Baranger M, Kuma K. Nucl. Phys. A, 1968, **122**: 241–272
17 Möller P, Nix J R. Nucl. Phys. A, 1992, **536**: 20–60
18 Castel B, Towner I S. Modern Theories of Nuclear Moments. Oxford: Clarendon, 1990
19 Strutinsky V M. Nucl. Phys. A, 1967, **95**: 420–442
20 Myers W D, Swiatecki W J. Nucl. Phys, 1966, **81**: 1–60
21 Raman S, Nestor Jr. C W, Tikkanen, P. At. Data Nucl. Data Tables, 2001, **78**: 1–128
22 Khoo T L, Waddington J C, O'Neil R A et al. Phys. Rev. Lett., 1972, **28**: 1717–1720
23 Sheikh J A, SUN Y, Walker P M. Phys. Rev. C, 1998, **57**: R26–R30
24 Purry C S, Walker P M, Dracoulis G D et al. Nucl. Phys. A, 1996, **632**: 229–274